3

Noise Limitations of Miniature Thermistors and Bolometers

Béla Szentpáli
Hungarian Academy of Sciences, Research Institute for Technical Physics and Materials Science, Hungary

1. Introduction

The miniature thermal resistors are comprehensively applied as thermistors or bolometers. Due to the dynamic development of the micromachining technologies became possible their mass-production with the precision and reproducibility of the microelectronics. These techniques result in typical lateral dimensions in the 1….100 μm range and thicknesses about μm, or less. The miniature devices fulfil the present-day requirements of the measuring and regulating systems demanding a large number of high-speed sensors for following quick changes, or for ensuring the quick read-out in integrated systems comprising many devices. However the higher working speed demands electronic processing circuits with broader bandwidth and consequently higher noise. Therefore it seems worth to reconsider the electronic noises of the miniature devices.

The phenomenological thermodynamic parameters depend on the average of the chaotic motion of the atoms and/or molecules. Therefore some fluctuations of their values are expected especially in very small volumes. This fact sets a physical limitation to the miniaturization; the size of the device should be large enough for representing the thermal parameters with the desired accuracy. According to the statistical physics (see eg. Kingston 1978) the mean square fluctuations of the energy is

$$\overline{\delta E^2} = kCT^2 , \tag{1}$$

where k, C and T are the Boltzmann constant, the heat capacitance of the volume under discussion and the absolute temperature respectively. Because $E = CT$, (1) can be rearranged:

$$\frac{\overline{\delta T^2}}{T^2} = \frac{k}{C} \rightarrow \frac{\delta T}{T} = \sqrt{\frac{k}{C}} \tag{2}$$

This criterion stands a lower limit to the dimensions of the miniature thermal sensors, but it is in the nanometre region. For example in 1 μm^3 platinum δT/T = 1,6*10^{-6} and similarly in 1 μm^3 Si δT/T = 2*10^{-6}. It depends on the application whether it is a practical limitation or not.

The temperature changes of the thermistor lead to changes of the resistance, as

$$r(T) = r_m(1 + \alpha(T - T_m)) = r_m(1 + \alpha\Delta T) , \tag{3}$$

where r and r_m are the electric resistance of the thermistor at temperatures T and T_m respectively. If the thermistor is driven by a constant current (i), then the temperature can be deduced from the voltage measured on it:

$$\Delta T = \frac{1}{\alpha} \cdot \frac{\Delta r}{r_m} = \frac{1}{\alpha} \cdot \frac{\Delta U}{U_0}, \tag{4}$$

where $U_0 = r_m * i$ is the voltage on the thermistor, when its temperature is T_m.

In this chapter the limitations of the achievable accuracy and resolution by the electronic noises are treated. These noises stand an ultimate limit of the performance besides the physical limitations. The three components of the resistor noises are considered: the thermal noise, the 1/f, or flicker noise and the generation-recombination noise occurring in semiconductors. The noise induced uncertainty monotonically increases with the bandwidth; therefore it seems worthwhile to reconsider this issue for the case of fast, miniature thermal resistors. In this chapter the electronic noise is considered in a bandwidth equal to the reciprocal value of the time constant of the heat relaxation:

$$\Delta f = \frac{1}{\tau}, \tag{5}$$

where Δf is the electronic bandwidth and τ is the characteristic relaxation time for the temperature changes. It was pointed out (Szentpáli, 2007) that the electronic processing having this bandwidth is a reasonable trade-off; such an electronics follow the $exp(-t/\tau)$ time relaxation with an accuracy of 5..15%. The accuracy improves approximately proportional with increasing bandwidth, but it grows worse quickly in narrower bandwidths.

2. Thermal model

Regarding the principal application the thermistors and the bolometers should be distinguished. The thermal equivalent circuits of them are shown in Fig.1.

In the thermistor case the thermal resistor is connected to a thermal reservoir, i.e. to a medium having much larger heat capacity than the probe itself. There is a thermal resistance between the reservoir and the thermal resistor. The thermal equivalent circuit of this situation and also the used notations is depicted in Fig. 1.a. The temperature of the reservoir holds the information on the interested physical quantity; therefore the aim is the precise measurement of T. In some applications the thermal resistance R is connected to the physical quantity, e.g. miniature Pirani type vacuum sensors (Berlicki, 2001), or similarly the thermal transfer between a heater and a temperature probe measures the flow rate of a gas, or liquid (Fürjes et al., 2004).

In equilibrium the temperature of the thermal probe, T_m is:

$$T_m = T - R\frac{T - T_A}{R + R_p} + R\frac{R_p}{R_p + R}P_i, \tag{6}$$

or

$$T - T_m = \frac{R}{R + R_p}(T - T_A - R_p P_i) \tag{7}$$

When T has a step–like change with ΔT«T, then the new equilibrium $T_m + \Delta T_m$ will set in exponentially:

$$T_m + \Delta T_m = T_m + (\Delta T - R\frac{\Delta T}{R + R_p}) \bullet (1 - e^{\frac{-t}{\tau_1}}), \tag{8}$$

where

$$\tau_1 = \frac{RR_p(C + C_P)}{R + R_p} = \frac{RR_p C^*}{R + R_p} \tag{9}$$

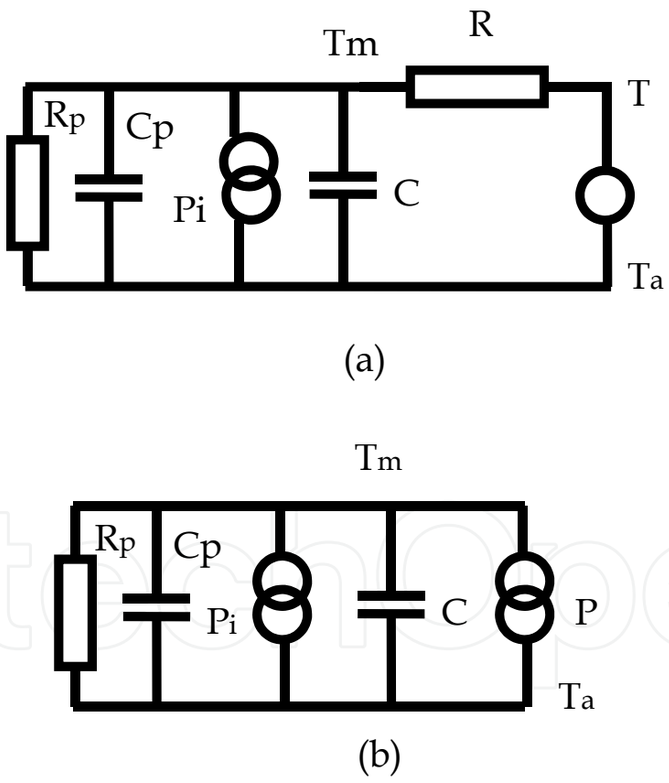

Fig. 1. The thermal equivalent circuits. (a) the thermistor configuration: the probe is connected to a thermal reservoir at temperature T; (b) the bolometer configuration: the probe absorbs the power P. Ta, Tm, C, Pi, Rp and Cp are the temperature of the ambient, the temperature of the probe, the thermal capacity of the probe, the power due to the read-out current, the thermal resistance and capacitance of the leads respectively.

For an ideal thermal probe R=0, and therefore T_m=T, τ_1=0. Further in this ideal case the Joule heating do not changes the T_m, so the read-out current on the resistor is not limited. Of course this configuration is not accomplishable. However, realistic measurements can be made only if R<<R_p. In this case:

$$\tau_1 \approx RC^* \tag{10}$$

It is obvious from (7) and (8) that the effect of the wires Rp, is reduced also if T_A is close to T. This can be achieved by thermalizing the leads and supports to a temperature close to T (Berlicki, 2001). The instant temperature can be observed only if τ_1 is small compared to the speed of the temperature changes.

The other configuration is the bolometer. In this case the measured quantity is power, which absorbs in the body of the thermal resistor. The equivalent circuit model is shown in Fig.1.b. Examples are: catalytic gas detectors (Bársony et al., 2004; Barocini et. al., 2004), radiation detectors (Almarsi et al. 2006; Graf et al. 2007). In equilibrium:

$$T_m = T_a + R_p(P + P_i) \tag{11}$$

If P has a step-like change with ΔP, then the new equilibrium T_m + Δ T_m will develop exponentially:

$$\Delta T_m(t) = R_p \Delta P(1 - e^{-\frac{t}{\tau_2}}), \tag{12}$$

where

$$\tau_2 = R_p(C + C_p) = R_p C^* \tag{13}$$

Other possible question is the response to a short power pulse which duration is small compared to τ_2. In this case:

$$\Delta T_m = \frac{\Delta E}{C^*} e^{\frac{-t}{\tau_2}}, \tag{14}$$

where ΔE is the total energy of the pulse.

The heat impedance of the losses trough the leads and supports are parasitic in the thermistor arrangement; however in the case of the bolometer configuration the role of R_p and C* are essential. A larger value of R_p increases the sensitivity; at the same time C* should be kept small for preserving the speed and the sensitivity for short pulses. Thin wires perform these two requirements simultaneously, however the electric resistance of them should be taken into account, or more wires (4 or 3) should be applied. Also the Joule heat in the thin current wires should be managed.

Albeit the equivalent circuit in Fig. 1. is the simplified description of the real structure, the R and C values basically can be calculated numerically from the parameters of the constructing materials and the geometry. In the case of extended dimensions (leads, supports) the calculations can be made on the basis of distributed network. Beyond the "a

priori" method these parameters can be deduced from measurements too. E.g. R could be determined as a limiting value of measurement series performed with successively increasing heat isolations on the probe. In general both τ values can be determined from the relaxation after a step like increment of P_i which occur remarkable heating up (Imran & Bhattacharyya, 2005).

In many cases the expressions in the frequency domain are more practical, instead of the time domain. The power spectral density of the exponential relaxation is the Lorentzian (see. e.g. Fodor, 1965):

$$e^{\frac{-t}{\tau}} \rightarrow \frac{\tau}{1+(\omega\tau)^2} \tag{15}$$

For example the power spectral density of the temperature fluctuations described by (2) is:

$$\delta\left(\Delta T^2\right)_f = \frac{4kT^2R}{1+\left(2\pi fCR\right)^2}, \tag{16}$$

where R is the heat resistance which connect the observed volume to the ambient. C is the heat capacitance of the volume under discussion, see (1), and (2). The relaxation time is τ=RC. Sometimes this noise is called "phonon noise", or fluctuation of the heat conductance.

If the heat capacitance and resistance cannot be considered as discreet elements, but distributed parameters along one dimension, then (Socher at al., 1998):

$$\delta(\Delta T^2)_f = \frac{16kT^2R'}{\pi L(R'G' + \frac{\pi^2}{4L^2})} \frac{1}{1+(\frac{2\pi fR'C'}{R'G' + \frac{\pi^2}{4L^2}})^2}, \tag{17}$$

where R'and C' are the heat resistance and the heat capacitance per unit length; G' is the heat conductance to the ambient per unit length and L is the length of the structure, considered as being one dimensional.

3. The thermal noise

The Nyquist, or Johnson noise is generated by the thermal motion of the electrons. This is a "white" noise, i.e. the noise power in unity bandwidth is constant, independent on the frequency. The cut off frequency at room temperature is in the terahertz region (Hooge et al., 1981). It occur voltage, or current fluctuations depending on the embedding circuit (van der Ziel, 1986). The variance of the voltage across the resistor terminals is:

$$\overline{\left(U-\overline{U}\right)^2} = \delta U^2 = 4kTr\Delta f, \tag{18}$$

where Δf is the bandwidth in which the noise is measured. The square root of the variance is the standard deviation, which is the so called "thermal voltage":

$$\delta U = \sqrt{4kTr\Delta f} \tag{19}$$

This voltage fluctuation is present on the resistor even without bias. Therefore the relative importance of the thermal noise is smaller when the useful signal increases, i.e. when the bias on the resistor is large. However, the bias is limited by the self-heating of the thermal resistor.

In the "thermistor" case an upper limit of the bias can be derived from the accuracy. The Joule heating results in temperature drop on R. The maximum of this drop can be prescribed as:

$$i^2 rR \le pTm\,, \tag{20}$$

where *i* is the biasing current and p is constant, which express the required accuracy. From (6) and (20) follows the maximum of the voltage drop on the resistor r:

$$U_0 = \sqrt{\frac{pr(R + R_p)T_m}{RR_p}} \tag{21}$$

Substituting (19) and (21) into (4) and taking into account (10) it gives:

$$\delta T_{th} = \frac{1}{\alpha}\frac{\delta U_{th}}{U_0} = \frac{1}{\alpha}\frac{\sqrt{4kTr/\tau_1}}{U_0} = \frac{2}{\alpha}\sqrt{\frac{kT}{pC^*T}} \tag{22}$$

This is the uncertainty of the temperature read-out due to the thermal noise if the bandwidth is $1/\tau_1$. It is worthy to note that this uncertainty does not depend on the actual value of r and R. Except the constants it depends only on the ratio of the thermal energy and the heat accumulated in the heat capacitance, C*.

For bolometer case the rearrangement (11) and (4) gives:

$$\delta P_{th} = \frac{\delta T_{th}}{R_p} = \frac{1}{\alpha R_p}\frac{\delta U}{U} = \frac{1}{\alpha R_p}\frac{\sqrt{4kT_m r/\tau_2}}{ir} = \frac{2\sqrt{kT_m}}{i\alpha R_p^{3/2}\sqrt{rC^*}} \tag{23}$$

In these measurements there is no need for accurate determination of temperature, therefore the choice of the bias current and the resistor temperature T_m depends on different considerations. E.g. the catalytic gas detectors work at temperatures about 700 ^oC, which is ensured by the bias current (Fürjes et al., 2002).

In the similar way from (14) it gives:

$$\delta E_{th} = \delta T_{th} C^* = \frac{C^*}{\alpha}\frac{\delta U}{U} = \frac{C^*}{\alpha}\frac{\sqrt{4kT_m r}}{ir\sqrt{R_p C^*}} = \frac{2\sqrt{kT_m C^*}}{i\alpha\sqrt{rR_p}} \tag{24}$$

For small incident powers, or energies T_m in (23) and (24) depends on the read out current. $T_m = T_0 + R_p i^2 r$. At elevated temperatures, when $T_m >> T_0$, the δP_{th} and δE_{th} become independent on the current according to (23) and (24). However, it should be noted that at elevated temperatures even some deterioration of accuracy can occur, because the value of α

decreases at high temperatures for the greatest number of materials. The increase of the current in the region, where it gives rise to only moderate temperature increment improves the accuracy.

4. The flicker (1/f) noise

The flicker or 1/f noise is also a general component in all resistors. It originates from the fluctuation of the resistance, concretely from the fluctuations of the mobility, or in other words from the fluctuations of the thermal scattering of mobile charge carriers (Kogan, 1996). Therefore this effect stands an absolute limit to the accuracy of the measurement; it can not overcome by increasing the bias. The spectrum of the 1/f noise is:

$$\frac{\delta r_f^2}{r^2} = \frac{C_{1/f}}{f} \tag{25}$$

The dimensionless number $C_{1/f}$ is the measure of the magnitude of the noise, δr_f^2 is the spectral density of the variance of the resistance, i.e. the variance measured in unity bandwidth. $C_{1/f}$ makes possible to compare the noise levels observed under different conditions as frequency ranges, current or voltage. In metallic and semiconductor resistors the Hooge-relation (Hooge, 1969) is valid:

$$C_{1/f} = \frac{\alpha_H}{N}, \tag{26}$$

where α_H is the so called Hooge-constant and N is the total number of mobile charge carriers in the resistor. The value of α_H is not universal constant, as it was supposed earlier, when Hooge discovered the above relationship. It varies from about 0.1 to 10^{-8} for different materials and structures (Kogan, 1996). Largest values of α_H were obtained in strongly disordered and inhomogeneous conductors, e.g in high-Tc superconductors, as it will be presented in section 9. As $C_{1/f}$ is able to compare different measurements, the Eq. (26) offers more general facility of comparison, because α_H is a specific material parameter, independent of the number of charge carriers, i.e. the volume of the resistor. Therefore not only the noises obtained under different measuring circumstances on equivalent resistors can be compared, but also noises of samples having different sizes. On other hand Eq. (26) shows that the noise is larger in smaller resistors made from the same material. It should be noted here that there are other 1/f noises too; e.g. in the channel of MOS transistors the 1/f noise is produced by fluctuation in number of electrons trapped in the oxide (Kingston (Ed.), 1957).

It should be realized that the spectrum cannot be exactly 1/f in the whole frequency range from zero to infinity. At first the spectrum is undefined at f=0, because the zero divider in (25). Further the total noise power, which is the integral of the spectrum is the logarithm function, which has infinite values when $f \to 0$ and when $f \to \infty$. Therefore it is generally assumed, that the spectrum flattens below a certain low frequency and it should be stepper over a certain high frequency. However, neither of this frequency limits have been observed yet. In spite of this fact the integration of the spectrum can be performed in a finite frequency region, which does not involve the 0 Hz (Szentpáli, 2007). The variance of the resistance is taken as:

$$\delta r^2 = r^2 C_{1/f} \int_{f_1}^{f_2} \frac{df}{f} = r^2 C_{1/f} \log_e \left(\frac{f_2}{f_1} \right), \tag{27}$$

where $f_2 = 1/\tau$ and $f_1 = f_2/a$, and expediently $a >> 1$. The relative fluctuation of the resistance is:

$$\frac{\delta r}{r} = \sqrt{C_{1/f} \log_e a} \tag{28}$$

It should be noted here that in this treatment of the 1/f spectrum that the noise in the bandwidth is independent on the frequency, it depends only on the ratio a. However due to the square root and log function, this dependence is rather weak. For sake of simplicity in this paper $a=10^6$ will be used. It means that

$$\frac{\delta r}{r} = 3.7 \sqrt{C_{1/f}} \tag{29}$$

As it was mentioned the choice of the "a" value is not decisive, e.g. taking only 3 decade bandwidth the multiplayer in (29) would be 2.6. Similarly 9 decade bandwidth results in a numeric factor of 4.5. Even the value of $C_{1/f}$ is not known with better accuracy. Suggestively the value of f_1 can be interpreted as the reciprocal of the time of observation. A numeric example: $a=10^6$ can mean that f_2=10 kHz is the upper cut-off frequency of the electronics belonging to 0.1 ms relaxation and $1/f_1$=100s is the time of the measuring.

The fact that the fluctuation due to the flicker noise is hardly sensitive to the bandwidth and unrelated to the absolute value of the frequency means that it is not worth to limit the speed of the electric circuit.

Substituting (29) into (4) we obtain the 1/f noise equivalent uncertainty of the temperature of the thermistor:

$$\delta T_{1/f} = \frac{3.7 \sqrt{C_{1/f}}}{\alpha} = \frac{3.7 \sqrt{\alpha_H}}{\alpha \sqrt{N}} = \frac{3.7 \sqrt{\alpha_H}}{\alpha \sqrt{nV}}, \tag{30}$$

where n is the volume density of free charge carriers and V is the volume.

For the bolometer configuration it gives

$$\delta P_{1/f} = \frac{\delta T}{R_p} = \frac{1}{R_p} \frac{3.7 \sqrt{\alpha_H}}{\alpha \sqrt{nV}} \tag{31}$$

The noise equivalent pulse uncertainty is:

$$\delta E_{1/f} = \delta T C^* = C^* \frac{3.7 \sqrt{\alpha_H}}{\alpha \sqrt{nV}} \tag{32}$$

Here it is worthy of note that the introduction of the integral (27) makes possible to express the figures of merit as δT, δP and δE on the basis of (26), which is a principal physical relation. The general conclusion on the 1/f noise is that the measuring circumstances practically cannot influence it. It can be influenced only by the construction, by the α_H value of the applied material and the volume. The increase of the volume decreases $\delta T_{1/f}$ and $\delta P_{1/f}$ at the sacrifice of the speed. $\delta E_{1/f}$ is proportional to C*~V, the 1/f uncertainty changes as $V^{-1/2}$, therefore finally $\delta E_{1/f}$ is proportional to $V^{1/2}$. In this case the smaller volume is clearly advantageous.

5. The generation-recombination noise

In semiconductor resistances the generation-recombination of mobile charge carriers from trap states give rise also to the fluctuations of the resistance. This type of noise is absent in metals, moreover plays no role in the present-day silicon material, which is practically free from deep centres. The probability of the emission from the trap state is exponential, while the recombination is obeyed by the mass-action law. The simplest case of the generation-recombination process is when there is only one trap centre, and then the related noise spectrum is the transformed exponential function: the Lorentzian, (Jones, 1994). This is shown in Figure 2 together with spectra of the other noises, mentioned earlier.

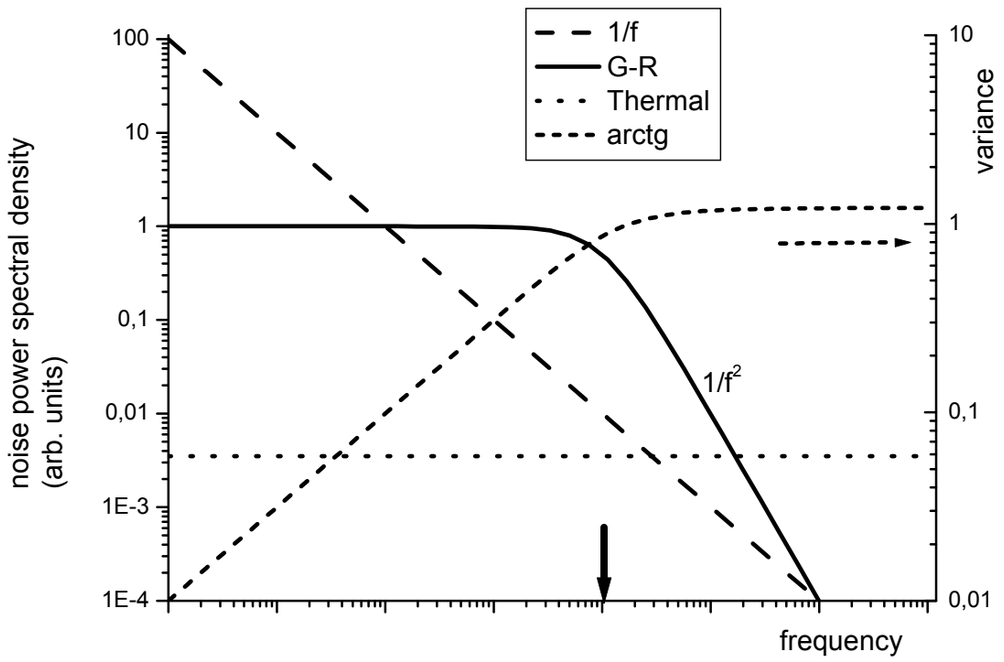

Fig. 2. The spectra of the different noises. The right hand scale is the variance of the g-r spectrum.

At low frequencies always the 1/f noise prevails over the other noise mechanisms, on the high frequency part of the scale the thermal noise dominates. The crossing point of the two spectra is about 1 kHz for such granular materials as the graphite and it sinks to 1 Hz region, or below for metals; for semiconductors this point is between the two values,

depending on the material and the doping. The breaking point of the Lorentzian spectrum of the generation-recombination (g-r) noise is $1/\tau$; it depends exponentially on the temperature. This noise can be observed in a wide frequency range, if there is a noticeable amount of traps.

The Lorentzian spectrum of this type of resistance noise is:

$$\frac{\delta r^2}{r^2} = \frac{M\tau_{g-r}}{1+(2\pi\tau_{g-r}f)^2}, \tag{33}$$

where $\tau_{g\text{-}r}$ is the characteristic g-r relaxation time, which is the harmonic mean of the emission and capture times of the trap. M is the magnitude of the spectrum. In the case of more than one trap the situation becomes rather sophisticated, the spectrum can be the sum of the characteristic spectra, or it can be a new Lorentzian with a mixed $\tau_{g\text{-}r}$ value [Hooge , 2002, 2003). This case is out of the scope of the present discussion. The variance of r obtained in a finite bandwidth is:

$$\frac{\delta r^2}{r^2} = \int_0^f \frac{M\tau_{g-r}}{1+(2\pi\tau_{g-r}f')^2}df' = \frac{M}{2\pi}\cdot arctg(2\pi\tau_{g-r}f) \tag{34}$$

This function is also depicted in Figure 2, at frequencies $f<<1/2\pi\tau_{g\text{-}r}$ it can be approximated by linear function, while at higher frequencies it approximates the saturation value $\pi/2$. The noise equivalent uncertainties can be calculated for the two cases separately.

At low frequencies the fluctuation is:

$$\frac{\delta r}{r} = \sqrt{M\frac{\tau_{g-r}}{\tau}}, \tag{35}$$

where $1/\tau$ is the noise bandwidth, it is equal to $1/\tau_1$ or $1/\tau_2$ are for the thermistors or for the bolometer cases respectively. The corresponding uncertainties are:

in the thermistor arrangement

$$\delta T_{g-r} = \frac{1}{a}\sqrt{\frac{M\tau_{g-r}(R+R_p)}{RR_pC^*}} \cong \frac{1}{a}\sqrt{\frac{M\tau_{g-r}}{RC^*}} \tag{36}$$

in the bolometer set-up

$$\delta P_{g-r} = \frac{1}{\alpha R_p}\sqrt{M\frac{\tau_{g-r}}{\tau_b}} = \frac{1}{\alpha R_p}\sqrt{M\frac{\tau_{g-r}}{R_pC^*}} \tag{37}$$

and for the energy pulse

$$\delta E_{g-r} = \frac{1}{\alpha}\sqrt{\frac{M\tau_{g-r}C^*}{R_p}} \tag{38}$$

At frequencies $f>>1/2\pi\tau_{g\text{-}r}$ the effect of the g-r noise saturates, because practically the whole spectrum is taken into account. In this case the uncertainties can be expressed similarly to (30), (31) and (32), only the numeric factor $3.7\sqrt{C_{1/f}}$ should be changed to $\sqrt{M}/2$.

Thus:

$$\delta T_{g-r} = \frac{\sqrt{M}}{2a} \tag{39}$$

$$\delta P_{g-r} = \frac{\sqrt{M}}{2aR_P} \tag{40}$$

$$\delta E_{g-r} = C^* \frac{\sqrt{M}}{2a} \tag{41}$$

6. The thermopile

The thermopiles are related to the bolometers; in many cases they can substitute each other. The common feature is the temperature change of the sensitive element; however the operation principle of the thermopile is based on the Seebeck effect. The sketch of a miniature thermopile fabricated by micromachining is shown in Fig. 3.

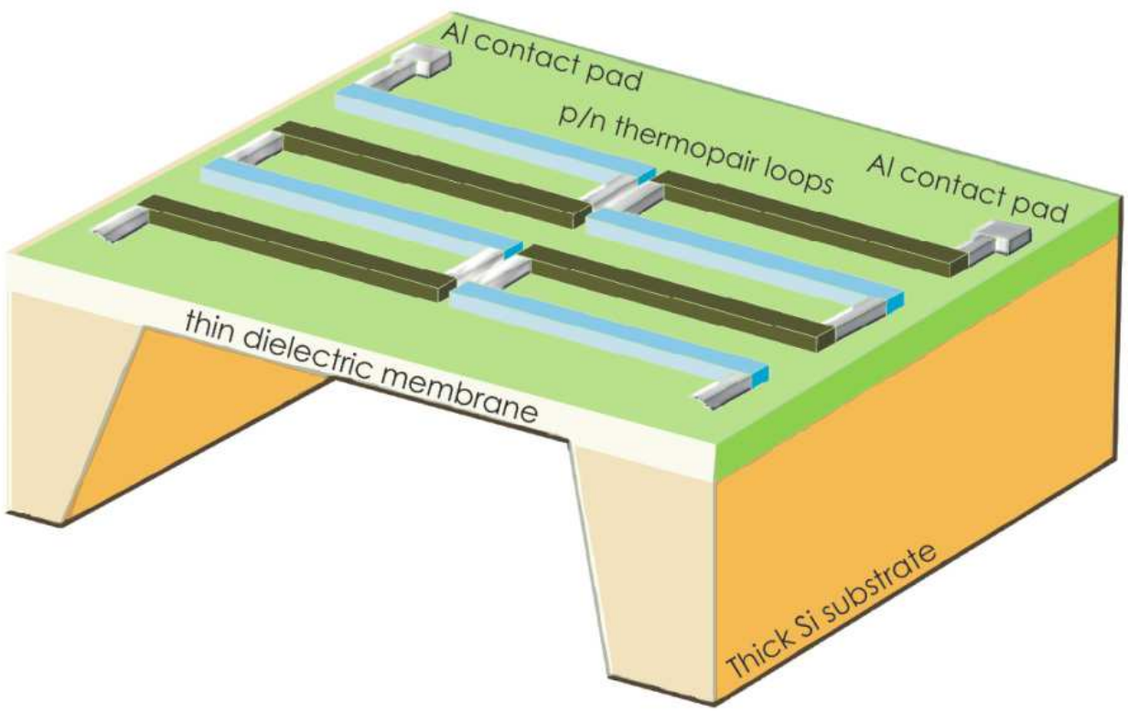

Fig. 3. The outline of a micromachined thermopile. The dimensions of the chip are in the mm range, the thickness and width of thermopair lines are typically in the sub micrometer and micrometer ranges respectively.

As it is obvious the miniature thermopile is not suitable to measure the absolute temperature; this task can be fulfilled by wire thermopairs; which is a well developed technique. The thermopiles sense the temperature difference; they can be applied for measuring the physical quantities which can be transformed to temperature difference (Graf et al., 2007). The absorbed power is such a quantity; it heats up more effectively the inner part of the thermopair loops, than the outer parts lying on the good heat conducting substrate. The strong thermal asymmetry is a key point of the operation. The central region on the membrane changes its temperature, while the outer parts lying on the good heat conducting substrate are thermalized to the ambient temperature. The serial connection of many thermopairs multiplies the output signal. Numerous different constructions are applied both as regards the materials and the geometrical construction. The micromachined thermopairs suitable can be produced by CMOS technology (Lenggenhager et al., 1992), in this case the one arm of the thermopairs is formed from p- or n- polycrystalline silicon and the other arm is aluminium in many cases. The alloys from different composition rates of Bi-Sb-Te are also popular due to their high Seebeck coefficient. Regarding the geometry there are closed membranes, as it is shown in Fig.3., beam-type membranes and a combination of the two the so called "bridge-type" membrane. These two latter constructions aim to increase the thermal resistance by reducing the contact between the membrane and the silicon rim. However the cantilever beam shaped membranes reduces the mechanical stability, and often become bent due to the different heat expansion coefficient of the multilayer structure. The bridge-type construction overcomes on this problem, the membrane is contacted on all sides to the substrate, but the contact areas are reduced. The thermopair configurations show also numerous variations. They can be arranged in parallel loops, or radial distribution. In some cases one strip lies upon the other. They are separated by a thin dielectric film; e.g. polycrystalline silicon - SiO_2 – Aluminium. Grouping the thermopairs linearly instead of loops the lines can act as miniature dipole antennas and the device detects the mm/THz waves (Szentpáli et al., 2010).

Because the output signal is the thermoelectric voltage measured by high impedance voltmeter there is no significant current in the thermopairs. Therefore the noises of the resistance – the 1/f fluctuation and the generation-recombination noise – play no role in this device. The important component of the noise is only the thermal noise of the resistor. The output voltage and also the electric resistance are proportional to the number of loops, however, the thermal noise voltage scales only to $\sim\sqrt{r}$, therefore the signal to noise ratio improves with increasing number of loops. If the area of the device is limited then sooner or later the number of the loops can be increased only by decreasing their widths. In this case the resistance will be proportional to the square of the number of the loops, and the signal to noise ratio will not improve, only the signal will be larger. However, it should be kept in mind that as the covering of the membrane grows the thermal resistance decreases and also the temperature difference on the thermopairs reduces in applications where the input power is fixed, e.g. radiation detectors, etc. The temperature distribution along the thermopair arms depends on the configuration and also on the excitation (Socher et al., 1998; Xu et al., 2010; Ebel et al., 1992). The common feature is the increment of the temperature difference with the length of the thermopairs. If the major heat conductance is through the

thermopair strips, then this dependence is quadratic, the cooling through the atmosphere and the heat loss through radiation decreases this dependence, but it remains super-linear. Therefore the increase of the length of the thermopairs will result in the improvement of the signal to noise ratio.

While the bolometers work under isothermal conditions, the output signal is the average of the effects in the volume. Therefore the temperature fluctuation described by (2) is practically smoothed to invisible. This is not trivial for thermopairs. Here the temperature and its gradient are distributed somehow along the sensor wires and even a small section can add a determining amount to the output voltage. Therefore it is worth to investigate this effect. The spectral distribution of the thermal fluctuations has maximum when $(2\pi fCR)^2 \ll 1$. In this case (16) can be simplified:

$$\delta\left(\Delta T^2\right)_f = 4kT^2R \ \ [\frac{K^2}{Hz}] \tag{42}$$

The corresponding spectral distribution of the output voltage fluctuation is $(\delta U)^2=S^2*\delta(\Delta T^2)$, where S [V/K] is the Seebeck coefficient of the conductor. It is noted here, that the absolute Seebeck coefficient of most of the conducting materials are determined, or it can be measured by coupling them to lead, which has a low and precisely known Seebeck coefficient as a function of temperature (van Herwaarden & Sarro, 1986). The voltage fluctuation on an elementary length dl is:

$$\delta(U^2)_f = S^2 4kT^2 \frac{dl}{A\sigma_{th}}, \tag{43}$$

where A and σ_{th} are the cross section area and the thermal conductivity of the wire respectively. This fluctuation can be compared by the thermal voltage fluctuation (18) of the same elementary length:

$$\delta_{th}(U^2)_f = \frac{\delta U^2}{\Delta f} = 4kTr = 4kT\rho\frac{dl}{A}, \tag{44}$$

where ρ is the electrical specific resistance of the material. The ratio of the two noises is:

$$M = \frac{\delta(U^2)_f}{\delta_{th}(U^2)_f} = \frac{S^2T}{\sigma_{th}\rho} \tag{45}$$

The values of M are listed in Table 1. for two metals and two differently doped Si at 300 K.

	ρ [Ωm]	S [μV/K]	σ_{th} [W/mK]	M
Platinum	$1.06*10^{-7}$	4.45	71	$7.9*10^{-4}$
Aluminum	$2.65*10^{-8}$	1.6	237	$1.2*10^{-4}$
silicon p =$10^{25}m^{-3}$	$1.0*10^{-4}$	644	150	$8.3*10^{-3}$
silicon n= $10^{21}m^{-3}$	$4.5*10^{-2}$	1958	150	$5.7*10^{-7}$

Table 1. The ρ, S, σ and M values for platinum, aluminum and differently doped silicons.

It seems that the statistical fluctuation of the temperature has a negligible effect besides the thermal noise. The ratio M increases proportionally to the temperature, because the temperature fluctuation is proportional to T^2, while the thermal noise growth with T only. Using the data of the table 1. as a rough estimation the M=1 ratio could be achieved only at that temperatures, where the materials are already melted, or vaporized.

7. Thermal radiation

The bolometers are very much employed for sensing the thermal radiation. This topic has a large literature (see eg. Hennini & Razeghi, 2002). In this frequent case, the fluctuation in the photon flux sets a physical limit to the accuracy. The power emitted by the thermal radiation in the half space is expressed by the Stefan-Boltzmann formula, multiplied by the emissivity of the body under discussion:

$$P = A\varepsilon\sigma_{S\text{-}B}T^4\,, \tag{46}$$

where A is the emitting surface, ε is the emissivity and $\sigma_{S\text{-}B} = 5.67*10^{-8}$ $Wm^{-2}K^{-4}$ is the Stefan-Boltzmann constant. The emissivity of the ideal black-body is ε =1. Realistic bodies are "grey", their emissivity is ε <1. As a thumb rule the emissivities of metals are ε~0.1…0.2 and for dielectrics ε~0.7…0.8. Still in more precise description the emissivity depends on the wavelength, ε=ε(λ) (Kruse et al., 1962) and also on temperature. The emissivity describes also the measure of the absorption; in equilibrium every body emits and absorbs the same amount of the radiation at each frequencies. The emissivity of miniature bolometers can be improved significantly by covering with a multilayer resonant layer structure (Liddiard, 1984, 1986 and 1993). This improving is successful also for thermopairs (Roncaglia et al., 2007). For the same purpose porous gold layers, so called gold black can be applied too.

The emission of photons is a random process governed by the Einstein-Bose statistics. The spectral fluctuations of the emitted power can be derived on this base (Kruse et al., 1962) as:

$$\delta P_r = 8A\varepsilon k\sigma_{S\text{-}B}T^5 \tag{47}$$

It is noted here that (47) describes the power spectral density in the function of the frequency of the radiation and not against the frequency of the electronics. The observed noise is the integral of (47) for the radiation transmission and detection region.

In an application there are minimum three different components: the body of which the temperature is detected, the sensor and the ambient. For this case:

$$\delta P = 8F_{(1\to 2)}A_1\delta_{(S-B)}\boldsymbol{\varepsilon}_1\boldsymbol{\varepsilon}_2T_1^5 + 8F_{(3\to 2)}A_3\boldsymbol{\varepsilon}_{(S-B)}\boldsymbol{\varepsilon}_3\boldsymbol{\varepsilon}_2T_3^5 + 8A_2\boldsymbol{\varepsilon}_{(S-B)}\boldsymbol{\varepsilon}_2\boldsymbol{T}_2^5\,, \tag{48}$$

where $F_{i\to j}$ are the view factors and the indexes 1, 2, 3 denotes the observed body, the sensor and the ambient respectively. In radiative heat transfer, a view factor $F_{i\to j}$, is the proportion of all that radiation which leaves surface *i* and strikes surface *j* (Lienhard IV & Lienhard V, 2003). Eq. (48) expresses the ultimate limit of all thermal radiation detectors. In the practical arrangement the sensor "views" mainly the observed object, therefore the first term in the right side of (48) is the greatest. This fact limits the possibility of decreasing the noise by cooling the sensor and/or the ambient.

8. Figures of merit

The δT_{th}, δP_{th} and δE_{th} means those values which are required to produce voltage on the thermistor equivalent to the electronic noise. If all the three mentioned noise mechanisms are significant as it is shown in Fig. 2., then the resulting uncertainty contribution should be calculated as the square root of the sum of variances of the independent fluctuations, e.g:

$$\delta P = \sqrt{\delta P_{th}^2 + \delta P_{1/f}^2 + \delta P_{g-r}^2} \tag{49}$$

and similar relation for δT and δE. Sometimes these values are called "nominal detectable signal", or noise-equivalent signal. The minimum detectable quantities are larger for two reasons: the significantly detectable amount should be over the noise floor at least by a factor of 2, or rather 2.5 if the definition of the tangential sensitivity (H.A. Watson, 1969) is applied; further due to the finite bandwidth the detected signal is not the instant peak value, it is attenuated to a certain degree.

The expressions are not completely unambiguous in the literature. Usually the term "sensitivity" is used for the temperature measurement and the phrase "responsivity" for the power sensing. This later is the input–output gain of a detector system, its dimension is V/W, or A/W depending on the output signal.

A further parameter is the bandwidth of the system. In this chapter the calculations were performed for the greatest rational bandwidth, specified by the temperature settling time. In the ordinary way the noise equivalent power/ temperature/energy is expressed for a 1 Hz bandwidth and the speed of the sensor is given independently.

For radiation detectors the "specific detectivity" is a widespread figure of merit. It is equal to the reciprocal of noise equivalent power (*NEP*), normalized to unit area and unit bandwidth:

$$D^* = \frac{\sqrt{A * \Delta f}}{NEP_{(1Hz)}}, \tag{50}$$

where A is the area of the photosensitive region of the detector, Δf is the effective noise bandwidth, and the NEP is the noise equivalent power in unit bandwidth. Of course this definition is unambiguous only in the case of "white noises", as the thermal noise; for the „colour noises" -the 1/f and the g-r noise - also the absolute value applied frequency should be defined. The common units of D* are $cmHz^{½}/W$. D* also called the Jones in honour to R. Clark Jones who defined this magnitude (Jones, 1949).

9. Superconducting bolometers

The resistance of the superconductors performs a very sharp change in the transition region. The transition temperature (Tc) of the superconducting metals fall in the cryogenic temperature region mostly at around, or above 1 K, for some special alloy it can be around 10 K. E.g. for $Mo_{0.6}Re_{0.4}$ the transition temperature is 12.6 K (McMillan, 1968). There is an other group of materials, the so-called high-Tc superconductors, where Tc is in the 80…130

K range; above the boiling point of liquid nitrogen (77 K). These compound materials consist of 4-6 different components, their crystal structure is typically tetragonal. The transition temperature depend also on the magnetic field and through that on the current flowing in the bolometer. Fig. 4. shows the resistance change in the transition region.

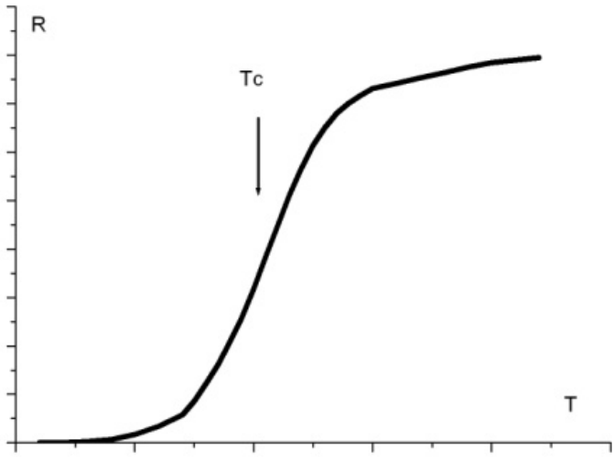

Fig. 4. The resistance in the transition region of superconductors. The axis are in arbitrary units.

The transition region is a few K for the high-Tc superconductors and only a few hundredths K for superconductors having transition temperature in the 1 K region. In the transition region the α is very high, it can overcome even the value of 5 (de Nivelle et al., 1997). These cooled bolometers are applied for sensing radiations; other applications fit hardly to the cryogenic surrounding. The setting into operation of the high-Tc bolometers is relative easy, because they can be cooled with liquid nitrogen or small cryocoolers. The cooling to around 1K , or even deeper needs big, sophisticated and expensive techniques. For both group of superconductors the effect of electrothermal feedback should be taken into account. The origin of this effect is the high value of α in the transition region. The functioning of the electrothermal feedback is shown in Fig. 5.

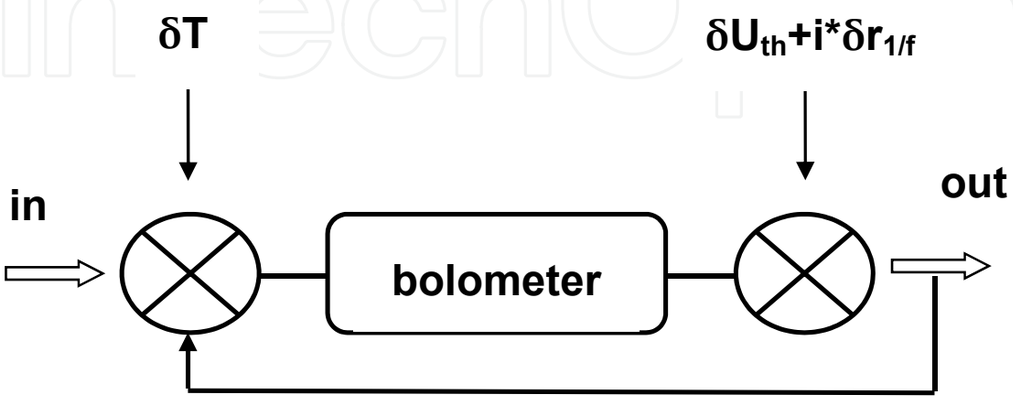

Fig. 5. The sketch of the electrothermal feedback, after de Nivelle et al., 1997.

The input radiation heats up the resistor therefore its resistance and voltage on it will increase if it is supplied by constant current. The higher voltage causes further dissipation and consequently heating. The feedback loop in the Fig. 5. takes account of this effect; the increment of the electric power dissipation adds up to the input signal. The gain of this loop is:

$$L = (P\alpha R_p) / \sqrt{1+(2\pi\tau_e)^2} = L_0 / \sqrt{1+(2\pi f\tau_e)^2}\,, \tag{51}$$

where P is the absorbed radiating power and $\tau_e = \tau_2/(1-L_0)$. The responsivity of the device is:

$$RES = \frac{1}{i}\frac{L_0}{1-L_0}\frac{1}{\sqrt{1+(2\pi f\tau_e)^2}} \quad [\frac{V}{W}] \tag{52}$$

For stable operation L_0 should be smaller than 1. In the literature L_0 = 0.3 is selected as an optimal value. If the bolometer is biased by constant voltage then L and RES become negative. In this case L_0 should be larger than -1 (de Nivelle et al., 1997).

The statistical fluctuation of the temperature (16) adds to the input, the equivalent power is:

$$P_{\delta T} = \frac{1}{R}\sqrt{\frac{4kT^2R}{1+(2\pi fCR)^2}} = \sqrt{\frac{4kT^2}{R(1+(2\pi fCR)^2)}} \tag{53}$$

The corresponding spectral density of the voltage noise power:

$$\delta U_{\delta T}{}^2 = RES^2\frac{4kT^2}{R(1+(2\pi fCR)^2)} \quad [\frac{V^2}{Hz}] \tag{54}$$

The thermal noise voltage (19) is added expediently to the voltage on the resistor. This increases the excess power dissipation by δV_{th} is: $\delta V_{th} i$. Finally, the thermal power spectrum of the thermal noise:

$$\delta U_{th}^2 = 4kTr(1+iRES) \tag{55}$$

The 1/f noise is the fluctuation of the resistance, see (25). It adds to the voltage δr*I. The power spectrum can be derived similar as above:

$$\delta U_{(1/f)}^2 = (\frac{riC_{(1/f)}}{f})^2(1+iRES) \tag{56}$$

The G-R noise is also the fluctuation of the resistance, it could be treated similarly, but it plays no role in the superconductors, at least there is no mention on it in the literature.

The $C_{1/f}$ value of metals and simple alloys is very small due to the enormously large concentration of the mobile electrons. Therefore the 1/f noise is practically absent in

bolometers having transition temperature in the 1…10 K range. However, the statistical fluctuation of the temperature can be observed (Maul et al., 1969).

The 1/f noise is significant in the high-Tc superconductors. The α_H values range from $5*10^{-4}$ to $1.4*10^{3}$ for different material compositions (Khrebtov, 2002). The epitaxial growth of the sensitive layer decrease the 1/f noise (de Nivelle et al. 1997), however, the α_H values show rather large scatter between the samples prepared in the same run, further α_H depends also on the α value in the same sample, i.e. it depends on the workpoint within the transition region. The noise spectrum fits to the $\sim 1/f^{\beta}$ characteristics with $\beta \sim 1$ from room temperature to the transition region; in the transition region the value of β changes between 0.8 and 2 (Khrebtov, 2002). In spite of these uncertainties the observation of the statistical fluctuations of the temperature was successful (de Nivelle et al., 1997). In general the high-Tc superconducting bolometers perform a remarkable progress as the improved technologies decrease the excess 1/f noise. The first published structure had $\alpha_H \sim 10^5$ and $D^* \sim 10^7$ cmHz$^{1/2}$/W, while in 2002 the best published data was $D^* = 1.8*10^{10}$ cmHz$^{1/2}$/W (Khrebtov, 2002).

10. Numeric examples

10.1 The pellistor

The first example is the "unsupported" pellistor, described in (Fürjes et al., 2002). It is applied for detection of combusting gases. This is a meander shaped resistor prepared from sputtered Pt film on the top of a SiO_2-SiN_x double layer from beneath the silicon substrate was removed (Dücső et al., 1997); see the photo in Fig. 6.a. It is used in bolometer regime, 18 mW electric input power heats it up to 780K. The heat capacitance is 41.57 nJ/K, the heat resistance to the surroundings is R_p = 26.9 K/mW, τ_2 = 1.15 ms. The electric resistance at 780 K is about 411 Ω and the measured thermal coefficient of the resistance $\alpha = 6.63*10^{-4}$ K^{-1}. The substitution of these data into (23) and (24) gives δP_{th} = 2.6 nW and δE_{th} = 2.9 pJ.

The effect of the 1/f noise can be taken into account by means of the $C_{1/f} = \alpha_H/N$ parameter. The measured α_H parameters of sputtered Pt films range from 10^{-4} to $2*10^{-3}$ (Fleetwood & Giordano, 1983). The published α_H values are related to the number of atoms instead of the number of conducting electrons. In this way the problems of the rather complex Fermi surfaces are skipped. The mass of this resistor is $2.33*10^{-8}$g. These data with the largest published α_H give $C_{1/f} = 2.8*10^{-17}$. The upper frequency limit of the bandwidth in the present case is in the kHz range; the integration in a bandwidth of six decades means that the lower limit falls in the mHz range. After substitution (31) and (32) give $\delta_{1/f}P$= 1 nW and $\delta_{1/f}E$= 1.2 pJ respectively.

The resulting noise: $\delta P = \sqrt{\delta P_{th}^2 + \delta P_{1/f}^2} = 2.8\,nW$, and $\delta E = \sqrt{\delta E_{th}^2 + \delta E_{1/f}^2} = 3.1\,pJ$, which are scarcely greater than the thermal noise, consequently even the pessimistically estimated 1/f noise plays no significant role under these circumstances. When the lateral dimensions of the device decrease by a factor of ten and the thickness of the platinum remains unchanged the electric resistance does not change and the volume of the resistor decreases by a factor of 100. In this case both δP_{th} and $\delta P_{1/f}$ increases ten times due to the decrease of C* and increase of $C_{1/f}$.

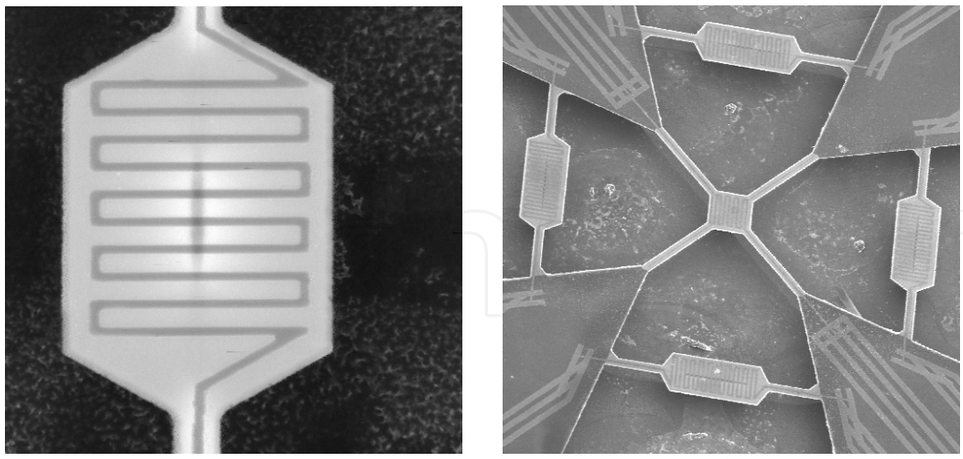

(a) (b)

Fig. 6. (a) The photo of the gas sensor pellistor, the size is 100x100 μm²; (b) the photo of the flow-meter chip.

10.2 The flow sensor

The photo of the device is shown in Fig.6.b. It consists of 4 bolometers described above and a central heater fabricated with the same technique. The gas (air) delivers the heat from the heater to the sensors by conductive and convective mechanisms. The heat transfer is equal to a heat resistance R~2 K/mW, at the flow velocity of 1 m/s. It is more than ten times less than $R_{p,}$; the τ_1 ~ 85 μs. The medium working temperature is 310 K, the electrical resistance 289 Ω, the thermal coefficient of the electrical resistance at this temperature is $\alpha=2.3*10^{-3}$ and the estimated value of $p=10^{-2}$. It is noted here, that the α value for sputtered metal layers are lower than that for well heat treated wires. From these data $\delta T_{th} \cong 0.88\, mK$. Substituting the above data in (30) the value of $\delta T_{1/f}$=0.029 mK is obtained. Also in this case The decrements of the lateral dimensions result in the simultaneous increase of both noises.

10.3 The implanted silicon resistor

The third example is an ion implanted Si resistor, measuring the temperature of the chip containing piezoresistive pressure sensors (Szentpáli et al., 2005). The parameters of the thermal resistor are not optimized for thermistor function; it was fabricated simultaneously with the piezoresistors, with the same B implantation step. The layout of the resistor is U shaped: two 150 μm long arms connected with a 40 μm bottom part. The width is 20 μm. The resulting doping profile is Gaussian, with a surface concentration of $6*10^{18}$ cm^{-3} and 2.3 μm depths. The resistors have a room temperature resistance of 2.3 kΩ, the temperature coefficient $\alpha=1.6*10^{-3}$ K^{-1}. The heat capacitance can be calculated from the geometrical data, it is C=25.5 nJ/ K. The heat resistance to the chip can be estimated from the electric spreading resistance. Between the p-type resistor and the n-type substrate there is a p-n junction. At large forward biases the I-V characteristics of the junction declines from the exponential due to the serial resistance. In the present case this resistance is 21Ω, and the analogous heat

resistance is about 5 K/W. The very low value of the heat resistance allow very quick work, τ_1=0.12 μs. (This is the reason of this indirect estimation of R, because a measurable heat relaxation would need too high heat pulse and precise resistance measurements at about 10 MHz bandwidth.) The connections between the resistor and the bonding pads are evaporated Al strips. Their temperature is equal to temperature of the chip, so the situation is similar to the previous one; the heat transfer from the thermistor to the leads is negligible. Supposing a 1 mA bias and the parameters used above (22) gives δT_{th}= 5 mK. (23) and (24) results in δP_{th}=1 mW and δE=127.5 pJ respectively. This device is a precise and very fast thermistor; however, the bolometer performance is limited by the low heat resistance R.

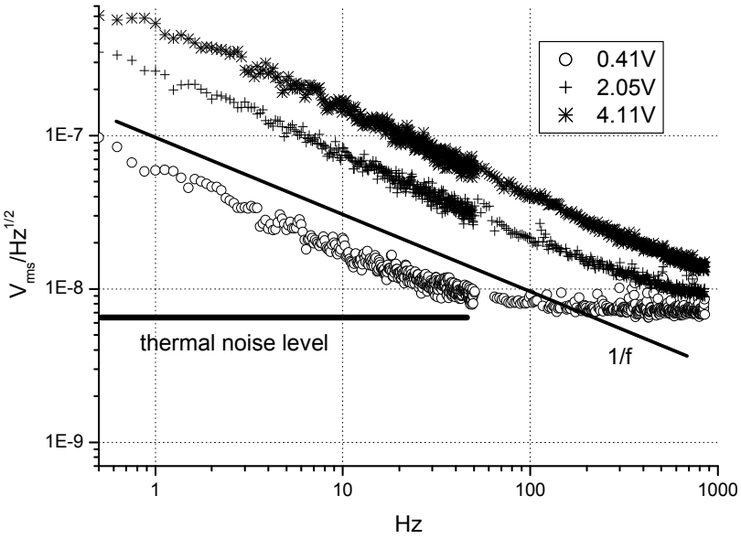

(a)

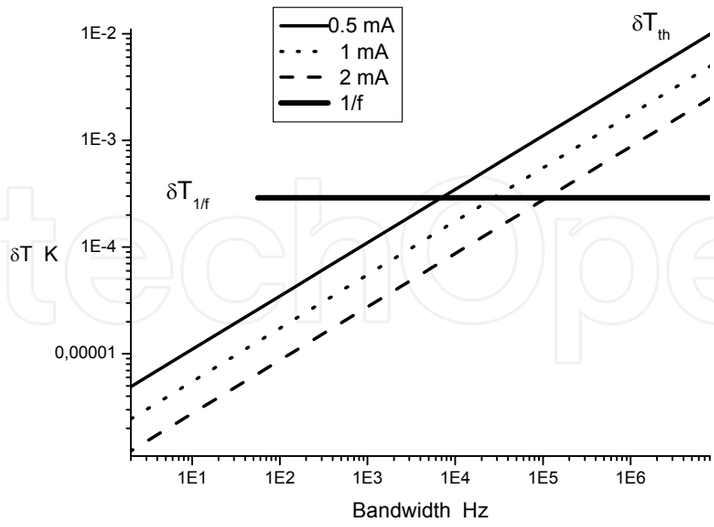

(b)

Fig. 7. (a) The measured noise spectra of the ion-implanted resistor. The continuous line stands for the 1/f characteristics; (b) Calculated δT_{th} and $\delta T_{1/f}$ at different biases and bandwidths.

The 1/f noise spectra of the resistor are shown in Fig.7.a. The spectra shift proportional to the bias, proving that the noise is caused by resistance fluctuations. From the spectra $C_{1/f}$ = $1.6*10^{-14}$ is obtained. Substituting this value in (30) $\delta T_{1/f}$ = 0.29mK, which is negligible comparing to the thermal noise. However most of the applications do not need so broad bandwidth, which is enabled by the thermal relaxations. If the electronic bandwidth is tighter, then δT_{th} will be smaller too and becomes comparable to the $\delta T_{1/f}$ or even sinks below it. In other words: the 1/f noise is the minimum of the total noise, which can be reached only in tight bandwidths. This is shown in Fig. 7.b.

11. Conclusions

The noise limited sensitivities of miniature thermal resistors were calculated. The statistical fluctuation of the temperature determines the lower limit of their size. The thermometer-type and the bolometer-type thermistor configurations were considered each with three different physical noise mechanisms: the thermal, 1/f and generation-recombination noises respectively. Special attention was put to the speeds of the measurements; which were limited by the thermal relaxations. The noise equivalent signals as δT in the thermometer configuration, δP and δE in the bolometer arrangement were calculated in the bandwidths limited by the thermal relaxations. It was shown, that under this circumstances $\delta T \sim \sqrt{k/C^*}$ and independent on the values of electric resistance and heat conductance. A method was proposed for the calculation of the noise equivalent signals from the spectra of the 1/f noise. The fluctuation in the thermal radiation set a physical limitation to the attainable accuracy, this effect was also treated. The thermopiles are closely related to the bolometers, it was shown that the main noise component in them is the thermal noise; they are free from the resistance fluctuations and in the practical cases the thermal noise exceeds the noise from the statistical fluctuation of the temperature. In the transition region of the superconducting bolometers the electrothermal feedback occurs due to the great thermal coefficient. The statistical fluctuation of the temperature is the main limitation of the performance of devices having Tc at deep temperature. The high-Tc superconductors show large 1/f noise, however they improve significantly with the development of the fabrication techniques. The statistical fluctuation of the temperature was observed even with such a bolometer. The numeric calculations of real miniature bolometers show that the practical limitations are due to the thermal noise. The 1/f noise becomes important only in semiconducting bolometers in small bandwidths.

12. Acknowledgment

This work was supported by the Hungarian Research Found (OTKA) under contract no.: 77843.

13. References

Almarsi, M., Xu, B. and Castrance, J. (2006). Amorphous silicon two-color microbolometer for uncooled IR detection. *IEEE Sensor J.* vol. 6. pp. 293-300

Barocini, M., Placidi, P., Cardinali G.C. and Scorzoni, A. (2004). Thermal characterization of a microheater for micromachined gas sensor. *Sensors and Actuators A*, 115 , pp. 8-14

Bársony, I., Fürjes, P., Ádám, M., Dücső, Cs., Vízváry, Zs., J. Zettner, J., and F. Stam, F. (2004). Thermal response of microfilament heaters in gas sensing, *Sensors and Actuators B*, vol. 103 , pp. 442-447. radiation detectors

Berlicki, T.M. (2001). Thermal vacuum sensor with compensation of heat transfer. *Sensors and Actuators A,* vol. 93, pp. 27-32

Chou B.C.S., Chen Y.M., Yang, M.O. and J.S. Shie, J.S. (1996). A sensitive Pirani vacuum sensor and the electrothermal SPICE modelling. *Sensors and Actuators A*, vol. 53, pp. 273-277

Dücső, Cs., Vázsonyi, É., Ádám, M., Szabó, I., Bársony, I., Gardeniers, J. G. E., van den Berg, A. (1997).Porous silicon bulk micromachining for thermally isolated membrane formation. *Sensors and Actuators A*, vol. 60, pp. 235-239

Ebel, T., Lenggenhager R. and Baltes, H. (1992). Model of thermoelectric radiation sensors made by CMOS and micromachining. *Sensors and Actuators A*, vol. 35, pp. 101-106.

Fleetwood, D. M. & Giordano, N. (1983). Resistivity dependence of 1/f noise in metal films. *Physical Review B*, vol. 27, pp. 667-671

Fodor, Gy. (1965). *Laplace Transforms in Engineering*, Publishing House of the Hungarian Academy of Sciences, Budapest

Fürjes, P., Vízváry, Zs., Ádám, M., Morrissey, A., Dücső, Cs. and Bársony, I., (2002). Thermal investigations of a microheater for micromachined gas sensor. *Sensors and Actuators A*, vol. 115, pp 98-103

Fürjes P., Légrádi G., Dücső Cs., Aszódi A. and Bársony I. (2004). Thermal characterisation of a direction dependent flow sensor. *Sensors and Actuators A*, vol. 115, pp. 417-423

Graf, A., Arndt, M., Sauer, M. and Gerlach G. (2007). Review of micromachined thermopiles for infrared detection. *Measuring Science and Technologies*, vol. 18, pp. R59-R75.

Hennini M. & Razeghi M. (2002). *Handbook of Infra-red Detection Technologies,* Elsevier, ISBN: 978-1-85617-388-9.

van Herwaarden, A.W., & Sarro, P.M. (1986). Thermal sensors based on the Seebeck effect. *Sensors and Actuators*, vol. 10. pp. 321-346.

F.N. Hooge F.N. (1969). 1/f noise is no surface effect. *Physics Letters*, vol. 29 A, pp. 139-140

Hooge, F.N., Kleinpenning T.G.M. and Vandamme L.K.J. (1981). Experimental studies on 1/f noise. *Rep. Prog. Phys.* vol. 44, pp. 479-532.

Hooge, F.N. (2002). On the additivity of generation-recombination spectra. Part 1: Conduction band with two centres, *Physica B*, vol. 311, pp. 238-249

Hooge, F.N. (2003). On the additivity of generation-recombination spectra. Part 2: 1/f noise. *Physica B*, vol. 336, pp. 236-251.

Imran M. & Bhattacharyya A. (2005). Thermal response of an on-chip assembly of RTD heaters, sputtered sample and microthermocouples. *Sensors and Actuators A: Physical*, vol. 121. pp. 306-320

Jones, R. C. (1949). Factors of merit for radiation detectors. *J. Opt. Soc. Am.* vol. 39, p. 344-356

Jones, B.K. (1994). Low-frequency noise spectroscopy, *IEEE Trans. On El. Dev*. vol. 41, pp. 2188-2197

Kingston R.H. (Ed.), (1957). *Semiconductor Surface Physics*, University Pennsylvania Press, Philadelphia

Kingston, R.H. (1978). *Detection of Optical and Infrared Radiation*, Springer-Verlag, New York.

Kogan, Sh. (1996). *Electronic noise and fluctuations in solids*, ISBN 0 521 46034 4, University Press, Cambridge

Khrebtov, I. A., (2002). Noise properties of high temperature superconducting bolometers. *Fluctuation and Noise Letters*, vol.2. pp. R51-R70

Kruse, P.W., McGlauchlin, L.D. and McQuistan, R.B. (1962). *Elements of infrared technology*.John Willey&Sons, New York, London

Leggenhager, R., Baltes, H., Peer, J. and Forster M. (1992). Thermoelectric Infrared Sensors by CMOS Technology. *IEEE Electron Device Letters*, vol. 13. pp. 454- 456.

Liddiard, K. C. (1984). Thin-film resistance bolometer IR detectors. *Infrared Phys*. vol. 24. pp. 57-64

Liddiard, K. C. (1986). Thin-film resistance bolometer IR detectors II. *Infrared Phys*. vol. 26. pp. 43-49

Liddiard, K. C. (1993). Application of interferometric enhancement to self-absorbing thin film thermal IR detectors. *Infrared Phys*. vol. 34. pp. 379-387

Lienhard IV, J.H. & Lienhard V, J.H. (2003). A *Heat Transfer Textbook.* Phlogiston Press, Cambridge, Massachusetts, U.S.A.

Maul, M.K., Strandberg M. W. P. and Kyhl, R. L. (1969). Excess noise in superconducting bolometers. Physical Review, vol. 182. pp. 522-525

McMillan, W. L. (1968). Transition temperature of srong-coupled superconductors. *Physical Review*, vol. 167, pp. 331-344

de Nivelle, M.J.M.E., Bruijn, M.P., de Vries R., Wijnbergen J. J., de Korte, P. A. J., Sánchez, S., Elwenspoed, Heidenblut, T., Schwierzi, B., Michalke, W. and Steinbeiss, E. (1997). Low noise high-Tc superconducting bolometers on silicon nitride nembranes for far-infrared detection. *Journal of Applied Physics*, vol. 82, pp. 4719-4726

Roncaglia, A., Mancarella, F. and Cardinali, G.C. (2007). CMOS-compatible fabrication ofthermopiles with high sensitivity int he 3-5 μm atmospheric window. *Sensors and Actuators* B. vol.125. pp. 214-223

Socher E., Degani, O. and Nemirovsky, Y. (1998). Optimal design and noise considerations of CMOS compatible IR thermoelectric sensors. *Sensors and Actuators*, vol. A 71, pp. 107-115.

Szentpáli, B., Ádám, M. and Mohácsy, T. (2005). Noise in piezoresistive Si pressure sensors. *Proc. of the SPIE vol. 5846*. pp. 169-179. Austin, TX.

Szentpáli, B. (2007). Noise Limitations of the Applications of Miniature Thermal Resistors. *IEEE Sensors Journal,* vol. 7, No. 9, pp. 1293-1299

Szentpáli, B., Basa, P., Fürjes, P., Battistig G., Bársony I., Károlyi, G., Berceli, T., Rymanov, V. and Stöhr, A. (2010). Thermopile antennas for detection of millimeter waves. *Applied Physics Letters* vol.: 96, 133507, [doi.: 10.1063/1.3374445].

H.A. Watson, H. A., (1969). Microwave semiconductor devices and their circuit applications. McGaw-Hill, New York, pp. 379-381

Xu, D., Xiong, B. and Wang, Y. (2010). Modeling of Front-Etched Micromachined Thermopile IR Detector by CMOS Technology. *Journal of Microelectromechanical Systems*, vol. 19, pp. 1331-1340.

van der Ziel, A., (1986) *Noise in Solid State Devices and Circuits*, Wiley-Interscience ISBN 0-471-83234-0

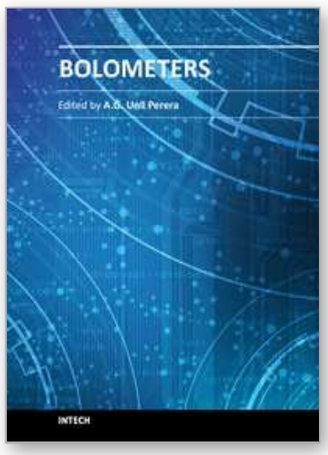

Bolometers

Edited by Prof. Unil Perera

ISBN 978-953-51-0235-9
Hard cover, 196 pages
Publisher InTech
Published online 09, March, 2012
Published in print edition March, 2012

Infrared Detectors and technologies are very important for a wide range of applications, not only for Military but also for various civilian applications. Comparatively fast bolometers can provide large quantities of low cost devices opening up a new era in infrared technologies. This book deals with various aspects of bolometer developments. It covers bolometer material aspects, different types of bolometers, performance limitations, applications and future trends. The chapters in this book will be useful for senior researchers as well as beginning graduate students.

How to reference

In order to correctly reference this scholarly work, feel free to copy and paste the following:

Béla Szentpáli (2012). Noise Limitations of Miniature Thermistors and Bolometers, Bolometers, Prof. Unil Perera (Ed.), ISBN: 978-953-51-0235-9, InTech, Available from: http://www.intechopen.com/books/bolometers/noise-limitations-of-miniature-thermistors-and-bolometers

INTECH
open science | open minds

InTech Europe
University Campus STeP Ri
Slavka Krautzeka 83/A
51000 Rijeka, Croatia
Phone: +385 (51) 770 447
Fax: +385 (51) 686 166
www.intechopen.com

InTech China
Unit 405, Office Block, Hotel Equatorial Shanghai
No.65, Yan An Road (West), Shanghai, 200040, China
中国上海市延安西路65号上海国际贵都大饭店办公楼405单元
Phone: +86-21-62489820
Fax: +86-21-62489821

IntechOpen